Polymer Journal, Vol. 14, No. 3, pp 233—240 (1982)

Cooperative Interaction on Side-Chain Motion of Poly(α-amino acid)

Shin YAGIHARA and Kunio HIKICHI

Department of Polymer Science, Faculty of Science, Hokkaido University, Nishi 8-chome, Kita 10-jo, Kita-ku, Sapporo 060, Japan.

(Received September 18, 1981)

ABSTRACT: Models of interacting side chains were proposed to explain the dielectric properties of poly(α-amino acid) in the solid state. Theoretical studies on these models were made by taking into account cooperative interactions among the side-chain motions. The theory explains the sudden change in dielectric loss with composition for copolymers of γ-methyl L-glutamate and γ-*p*-chlorobenzyl L-glutamate. The ranges of cooperative side-chain motion for these copolymers were estimated to be about 11 side chains. This value was compared with each of those of polymer blends of poly(γ-methyl L-glutamate) and poly(γ-*p*-chlorobenzyl L-glutamate). Differences in dielectric property between the copolymer and the polymer blend are explained by the effective free-volume on the basis of these models. Characteristics of cooperative interactions in chain motions of poly(α-amino acid)s and amorphous polymers were discussed.

KEY WORDS Cooperative Interaction / Poly(α-amino acid) / Amorphous Polymer / Side-Chain Motion / Dielectric Relaxation / Coaxial Two-Phase Model / Free Volume /

Cooperative properties of molecular motion are of importance in understanding the dynamical behavior of macromolecules[1-3] and small molecules as well.[4-6] It has been well established that the glass-rubber relaxation of conventional amorphous polymers is caused by cooperative motions of the main chain.[7-9] On the other hand, the side-chain motion has been considered to be less cooperative.[7,8,10] It has been reported that the side-chain relaxation of α-helical poly(α-amino acid) in the solid state resembles the glass-rubber relaxation of conventional amorphous polymers.[11-14] Side chains of γ-methyl L-glutamate (MLG) and γ-benzyl L-glutamate (BLG) in the copolymer of MLG and BLG undergo cooperative motions and show a single side-chain relaxation.[13] However, the cooperativity of the side-chain motion of poly(α-amino acid) seems to be less significant than that of the main-chain motion in conventional amorphous polymers.[15]

In our previous paper,[15] the dielectric properties of copolymers of MLG and γ-*p*-chlorobenzyl L-glutamate (*p*ClBLG) in the solid state were reported. We found that the dielectric properties did not change smoothly but rather abruptly with composition. Two side-chain relaxations related to MLG and *p*ClBLG side-chains, respectively, were observed for copolymers with mole fractions of *p*ClBLG ranging from 0.1 to 0.5. The value of the dielectric loss related to MLG side-chains was much smaller than that expected from the mole fraction of MLG residues in the copolymer. Thus, we suggest that the relaxation due to MLG side-chains in the copolymer is caused not by a single MLG side-chain, but by clusters of MLG side-chains larger than a certain critical size. In a cluster smaller than the critical size, the motion is severely restricted because of the interaction with *p*ClBLG side-chain. This cooperative property of the side-chain motion has not as yet been discussed in detail.

In the present paper, we present models to explain the cooperative property of the side-chain motion together with some theoretical considerations on the experimental results. Furthermore, we show dielectric data for blends of poly(γ-methyl L-glutamate) (PMLG) and poly(γ-*p*-chlorobenzyl L-

glutamate) (P*p*ClBLG) in order to test the models.

MODELS OF INTERACTING SIDE CHAINS

The side-chain relaxation of the α-helical poly(α-amino acid) in the solid state has been explained in terms of the coaxial two-phase model[16] which consists of a rigid main-chain core and a flexible side-chain region surrounding the core. This model suggests that the side-chain motion is affected by the side chain–side chain and the intramolecular backbone–side chain interactions.[17] The side chain–side chain interaction provides cooperative properties to motions of the side chains. When a copolymer is composed of two different side chains with different mobilities, the relaxation process reflects the cooperative interaction between side chains.

In the following, we consider two cases of copolymers and random mixtures of two homopolymers.

One-Dimensional Model for Copolymers

(i) *Random Copolymers.* In the case of a random copolymer of MLG and *p*ClBLG, two kinds of side chains MLG ('*m*') and *p*ClBLG ('*p*') are distributed randomly in the side-chain region of the coaxial two-phase model. Three assumptions are made. First, we assume that the distribution of side chains in the side-chain region is approximately one-dimensional, as shown in Figure 1a. It should be noticed that adjacent side chains in the sequence are composed not only of the side chains in the same molecule but also of the side chains of the neighboring molecules. Since the backbone takes the rigid structure, the intramolecular and intermolecular interactions between the side chains are indistinguishable. Secondly, we assume that both '*m*' and '*p*' side-chains can be either in the '*m*' or '*p*' motional states. Here '*m*' and '*p*' motional states refer to those of the '*m*' and '*p*' side-chains in the respective homopolymer. In the case of copolymer, the '*m*' and '*p*' motional states relate to the relaxations observed at higher and lower temperatures, respectively. Thirdly, we assume that in a cluster of '*m*' side-chains larger than the critical size n_1 (>1), '*m*' side-chains assume the '*m*' motional state, and that '*p*' side-chains adjacent to that cluster also assume the '*m*' motional state. All other side chains take the '*p*' motional state. Hereafter, N_{mm}, N_{pm}, etc. refer to the number of '*m*' side-chains in the '*m*' motional state, '*p*' side-chains in the '*m*' motional state, etc. We calculate the ratio R_1 of the number of side chains in the '*m*' motional state ($N_{mm}+N_{pm}$) to the total number of side chains N. The probability density $f_1(l)$ that l consecutive '*m*' side-chains terminated on both ends by a '*p*' side-

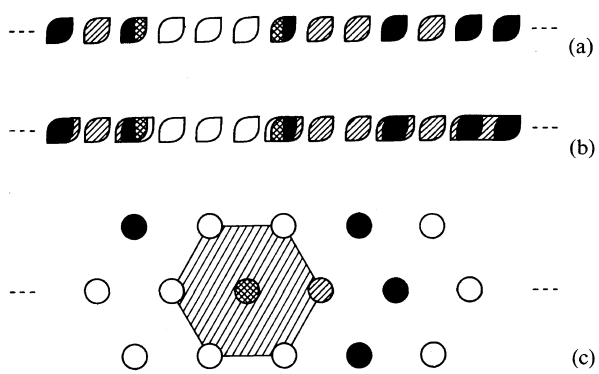

Figure 1. Examples of sequence models for
(a) a random copolymer of '*m*' and '*p*' with $n_1=3$: ( ) '*m*' side-chain in '*m*' motional state; ( ) '*m*' side-chain in '*p*' motional state; ( ) '*p*' side-chain in '*m*' motional state; ( ) '*p*' side-chain in '*p*' motional state.
(b) Konishi-Hatano model[19] with $n_{1K}=3$. Symbols have the same meaning as (a).
(c) random blend of 'P_m' and 'P_p' with $n_2=2$: (○) 'P_m' side-chain in 'P_m' motional state; (◍) 'P_m' side-chain in 'P_p' motional state; (◉) 'P_p' side-chain in 'P_m' motional state; (●) 'P_p' side-chain in 'P_p' motional state. Shaded region is considered.

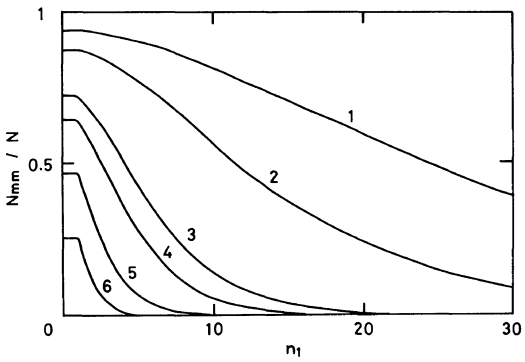

Figure 2. Plots of N_{mm}/N against n_1 at various mole fractions. Number represents the corresponding sample code.

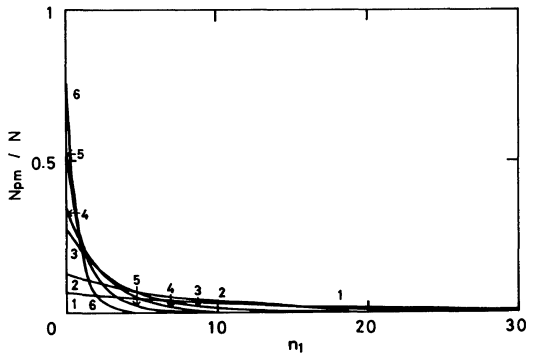

Figure 3. Plots of N_{pm}/N against n_1 at various mole fractions. Number represents the corresponding sample code.

Table I. Mole fraction of *p*ClBLG for each sample

Sample	Code	Mole fraction of *p*ClBLG
PMLG	—	0
Copolymer of MLG	1	0.06
and *p*ClBLG	2	0.12
	3	0.28
	4	0.35
	5	0.53
	6	0.75
P*p*ClBLG	—	0.99
Blend of PMLG	I	0.15
and P*p*ClBLG	II	0.40

chain occurs in the copolymer is written,

$$f_1(l)=\phi^l{}_m\phi_p^2\,, \tag{1}$$

where ϕ_m and ϕ_p are mole fractions of '*m*' and '*p*' side-chains, respectively. If N is infinitely large, the ratio of N_{mm} to N is described as,

$$N_{mm}/N=\sum_{l=n_1}^{\infty} f_1(l)l\,,$$

$$=(1-n_1)\phi_m^{(n_1+1)}+n_1\phi_m^{n_1}\,. \tag{2}$$

Equation 2 is shown in Figure 2 as a function of n_1 at six mole fractions ϕ_m corresponding to the present copolymers. The numbers described in the figure represent the copolymer codes in Table I. With increasing critical size n_1, this ratio decreases.

Next, we calculate the number of '*p*' side-chains in the '*m*' motional state, N_{pm}, which is equal to the number of clusters of '*m*' side-chains larger than n_1. Thus, N_{pm}/N can be calculated as follows,

$$N_{pm}/N=\sum_{l=n_1}^{\infty} f_1(l)\,,$$

$$=\phi_m^{n_1}(1-\phi_m)\,. \tag{3}$$

Figure 3 shows the n_1 dependence of N_{pm}/N, indicating that it is not appreciable at large n_1. Furthermore, the number of consecutive '*p*' side-chains in the '*m*' motional state is considered to be negligibly small except for $n_1 \lesssim 3$.

The ratio R_1 of the number of side chains in the '*m*' motional state to the total number is given by,

$$R_1=(N_{mm}+N_{pm})/N$$
$$=-n_1\phi_m{}^{(n_1+1)}+(1+n_1)\phi_m{}^{n_1}$$
$$=-n_1(1-\phi_p)^{(n_1+1)}+(1+n_1)(1-\phi_p)^{n_1}\,. \tag{4}$$

The value of R_1 is plotted against n_1 for six ϕ_p in Figure 4. Figure 5 shows the composition dependence of R_1 at five critical sizes n_1. The figure indicates that at larger n_1 the value of R_1 decreases more abruptly at lower values of ϕ_p, in agreement with the experimental results for the copolymers.

(ii) *The Konishi–Hatano Model.* As described in our previous paper,[15] no nuclear magnetic resonance spectra are available for copolymers of MLG and *p*ClBLG.[18] Konishi and Hatano[19] reported that in the copolymer prepared by the ester exchange reaction of PMDG and *p*-chlorobenzyl alcohol, the MDG residues and the units constituting a *p*ClBLG residue and the neighboring 0.5 MDG residue are

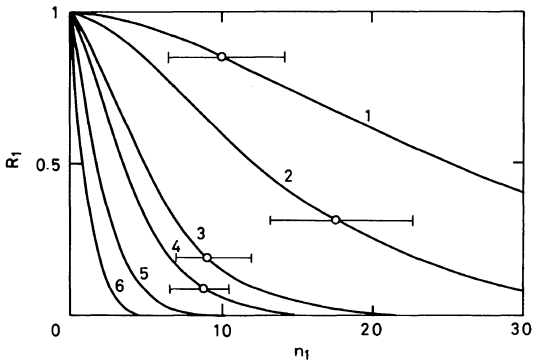

Figure 4. Plots of R_1 against n_1 for various mole fractions. Number represents the corresponding sample code. Circles show values calculated from eq 11. Error bars represent the conditions of eq 12 and the error of 3% in the separation of the relaxation curve.

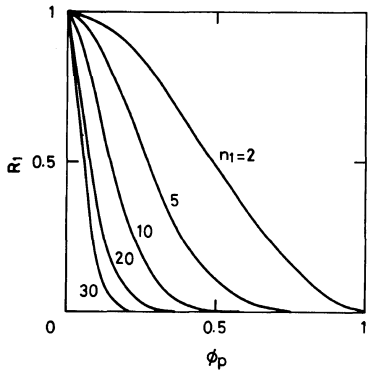

Figure 5. Composition dependence of R_1. Number represents the critical size n_1.

randomly distributed in the chain when $0<\phi_p<0.5$, as shown in Figure 1b. This 0.5 MDG residue is relatively small, and does not affect our model significantly.

Assuming the sequence reported by Konishi and Hatano, we obtain,

$$f_{1K}(l)=\phi_{mK}^{(l-0.5)}\phi_{pK}^2 \tag{5}$$

with ϕ_{mK} and ϕ_{pK} are defined by

$$\phi_{mK}=(1+\phi_m)/(3-\phi_m)$$

$$\phi_{pK}=\phi_p/(1+0.5\phi_p)$$

The fraction of the number of side chains in the 'm' motional state is given by,

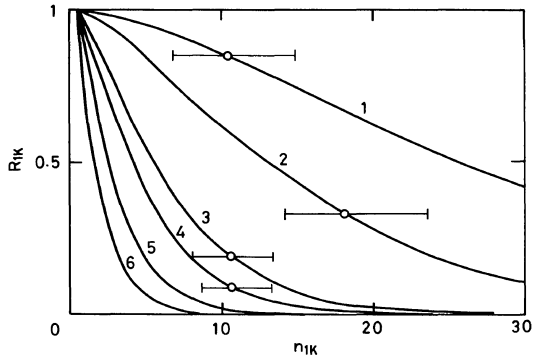

Figure 6. Plots of R_{1K} against n_{1K} for copolymers of MLG and *p*C1BLG. Circles and error bars have the same meaning as Figure 4.

$$\begin{aligned}R_{1K}&=(N_{mm}+N_{pm})/N\\&=2\phi_m[(1-n_{1K})\phi_{mK}^{(n_{1K}+0.5)}\\&\quad+n_{1K}\phi_{mK}^{(n_{1K}-0.5)}]/(1+\phi_{mK})+\phi_p\phi_{mK}^{(n_{1K}-0.5)}\end{aligned} \tag{6}$$

where n_{1K} is the critical size for cooperative motion in the Konishi–Hatano model. Values of R_{1K} are shown in Figure 6, which displays the similar behavior to that shown in Figure 4.

Two-Dimensional Model for Random Polymer Blend

We assume that two homopolymers 'P_m' and 'P_p' are randomly packed in a hexagonal net, whose cross section is illustrated in Figure 1c. We consider the shaded region which consists of the central molecule and six surrounding molecules. This cross section represents the whole side-chain region surrounding the same molecule. It should be noted that

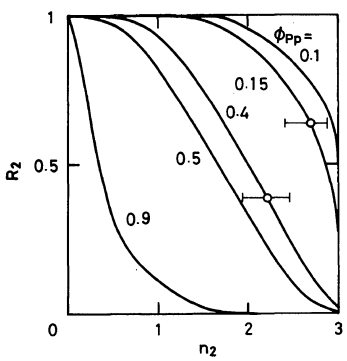

Figure 7. Plots of R_2 against n_2. Mole fractions are shown in the figure. Circles show values calculated from eq 11. Error bars have the same meaning as Figure 4.

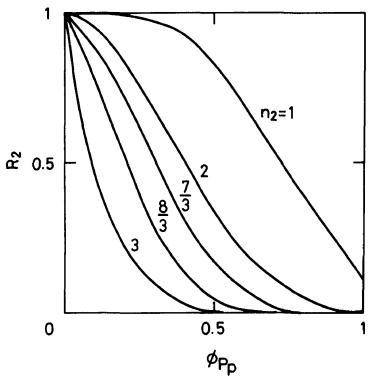

Figure 8. Composition dependence of R_2. Number represents the critical size n_2.

the central molecule gives the full contribution to this region, whereas a molecule at the corner of the hexagon makes only a one-third contribution. Thus, the number of side chains involved in this region is given by an integral multiple of one third, and varies from 0 to 3. We assume that if the number of 'P_m' side-chains exceeds a certain value n_2 ($=0$, $1/3$, $2/3, \cdots$, $9/3$), all side chains in this region take the 'P_m' motional state.

The probability density, $f_2(M)$ that M 'P_m' side-chains exist in this region is written as,

$$f_2(M)=\begin{cases} {}_6C_{3M}\phi_{P_m}^{3M}\phi_{P_p}^{(7-3M)}, & 0\leq M<1 \quad (7a) \\ {}_6C_{3M}\phi_{P_m}^{3M}\phi_{P_p}^{(7-3M)}+{}_6C_{3M-3}\phi_{P_m}^{(3M-2)}\phi_{P_p}^{(9-3M)}, & \\ & 1\leq M\leq 2 \quad (7b) \\ {}_6C_{3M-3}\phi_{P_m}^{(3M-2)}\phi_{P_p}^{(9-3M)}, & 2<M\leq 3 \quad (7c) \end{cases}$$

where ${}_6C_{3M}$ and ${}_6C_{3M-3}$ denote the binominal coefficients, and ϕ_{P_m} and ϕ_{P_p} are the mole fractions of 'P_m' and 'P_p' molecules, respectively. Equation 7a and the first term in the right-hand side of eq 7b are related to the case in which the central molecule is 'P_p', and the other terms to the case in which the central molecule is 'P_m'. The ratio R_2 of the number of side chains in the regions in which there are more 'P_m' side-chains than n_2 to the total number of side chains is thus obtained as,

$$R_2=\sum_{M=n_2}^{3} f_2(M) \quad (8)$$

This ratio is shown for five mole fractions in Figure 7 as a function of n_2. The composition dependence of R_2 at five n_2 is shown in Figure 8.

EXPERIMENTAL RESULTS

The results of dielectric measurements for the copolymers of MLG and *p*ClBLG were reported in the previous paper.[15] Here, we present the results for the blends of PMLG and P*p*ClBLG. Two blends of PMLG and P*p*ClBLG were cast from mixtures of concentrated chloroform solutions of PMLG and P*p*ClBLG at given mole fractions. The mole fractions ϕ_p is listed in Table I with those of the copolymers of MLG and *p*ClBLG with $0<\phi_p<0.75$. Preparations of the polymers and the experimental procedures have been also described previously.[15]

Figure 9 shows the temperature dependence of the dielectric loss ε'' for the blends of PMLG and P*p*ClBLG. Two relaxation processes corresponding to PMLG and P*p*ClBLG are observed. The relaxation related to PMLG does not shift to lower temperature with increasing ϕ_p, though we found such a shift in the copolymer. The dielectric loss related to PMLG is smaller than that expected from the PMLG mole fraction in the blend. However, the deviation is not as remarkable as that observed in the copolymer.

DISCUSSION

Separation of Two Relaxation Processes

Two relaxation processes brought about by the side chains in the '*m*' and '*p*' motional states for the copolymers could not be separated in the frequency domain. Thus, we attempted to separate these processes in the temperature domain by the following procedure. The relaxation curve of PMLG was scaled to the corresponding relaxation curve of a copolymer which was shifted along the temperature axis. Subtracting the scaled PMLG curve from the whole curve of the copolymer, we obtained the relaxation curve caused by the side chains in the '*p*' motional state. Though the procedures of scaling and shift were made as the curve related to the '*p*' motional state exhibited a smooth line, the separation remained ambiguous, because the procedures are correlated to each other. The maximum values of the resulting loss curves do not change very much, while the temperature of the maximum does. An example of this separation is shown in Figure

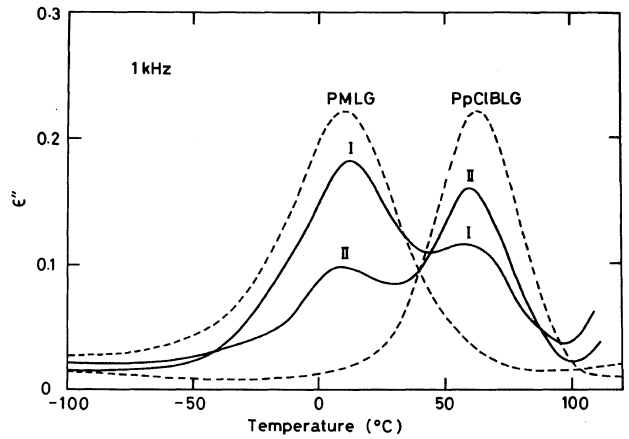

Figure 9. Temperature dependence of dielectric loss ε'' at 1 kHz for the blend of PMLG and P*p*ClBLG. The number represents the sample code.

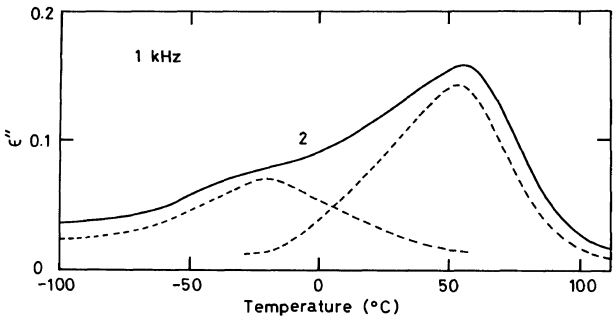

Figure 10. An example of the separation of two relaxation processes for copolymer 2. Dotted lines show two processes brought about side chains at the '*m*' and '*p*' motional state, respectively, at lower and higher temperature regions.

10.

For the polymer blend, we synthesized the relaxation curves of PMLG and P*p*ClBLG at a given ratio without any shift along the temperature axis, and scaled so as to fit the curve of the polymer blend.

Estimation of R_e

We estimated the ratio R_e of the number of side chains in the '*m*' motional state to the number of the total side chains in the copolymer using our experimental data. We used the value of maximum dielectric loss instead of the relaxation strength which cannot be evaluated because of the double-peak structure. It should be noted that the change in the shape of the dielectric loss curve shown in Figure 3b of ref 15 is caused by the difference between the apparent activation energy of the side-chain motion in the '*m*' motional state (30 kcal mol^{-1}) and that in the '*p*' motional state (50 kcal mol^{-1}). It is reasonable to assume that the whole curve is composed of two relaxation curves, the respective shape remaining unchanged. The maximum values of the dielectric loss obtained from both the temperature and frequency dependences were examined for PMLG and P*p*ClBLG, and the discrepancy between the two methods was estimated to be less than 1%. Thus the use of maximum dielectric loss obtained from the temperature dependence is considered to be a good approximation. Two extreme cases were considered: relaxation strengths per side chain in the '*m*' and '*p*' motional states are equal to those of PMLG and P*p*ClBLG, respectively, and the reverse case. In the first case,

the value of R_e is written as,

$$R_e=\frac{(\varepsilon''_m/\varepsilon''_{PMLG})N_{PMLG}}{(\varepsilon''_m/\varepsilon''_{PMLG})N_{PMLG}+(\varepsilon''_p/\varepsilon''_{PpClBLG})N_{PpClBLG}} \quad (9)$$

where ε''_m and ε''_p are the maxima of the dielectric loss at a frequency of 1 kHz for relaxations due to side chains in the '*m*' and '*p*' motional states in the copolymer, ε''_{PMLG} and ε''_{P_pClBLG} are those of PMLG and P*p*ClBLG, and N_{PMLG} and N_{P_pClBLG} are the numbers of MLG and *p*ClBLG side-chains per unit volume of the respective homopolymers. In contrast to this, in the second case, R_e is given by,

$$R_e=\frac{(\varepsilon''_m/\varepsilon''_{PpClBLG})N_{PpClBLG}}{(\varepsilon''_m/\varepsilon''_{PpClBLG})N_{PpClBLG}+(\varepsilon''_p/\varepsilon''_{PMLG})N_{PMLG}} \quad (10)$$

If we assume that the relaxation strengths per side chain for the '*m*' and '*p*' side-chains in either motional state are simply equal to those of PMLG and P*p*ClBLG, respectively, the real case will be somewhere between the above two extreme cases. Substituting the experimental value of 0.22 (shown in Figure 9) into the values of ε''_{PMLG} and ε''_{P_pClBLG}, R_e is obtained,

$$R_e=\frac{\varepsilon''_m}{\varepsilon''_m+\varepsilon''_p\gamma} \quad (11)$$

Here, γ is a parameter between N_{P_pClBLG}/N_{PMLG} and N_{PMLG}/N_{P_pClBLG}. These ratios were estimated from the densities calculated from spacings of X-ray photographs of respective homopolymers.[15] Thus, for γ we obtain,

$$\frac{N_{PpClBLG}}{N_{PMLG}}=0.6\leq\gamma\leq\frac{N_{PMLG}}{N_{PpClBLG}}=1.7 \quad (12)$$

Although the separation of two relaxations is somewhat ambiguous, we can obtain the value of R_e within an error less than 3% at a given value of γ.

Comparison of Experimental Results with Theory

(i) *Copolymer of MLG and pClBLG.* An estimated value of R_e at $\gamma=1.0$ is plotted for each copolymer in Figure 4. For copolymer 1, the value ε''_m is estimated from the broadness of the absorption curve. An uncertainty of R_e is shown as an error bar taking account of eq 12 and the error of 3% involved in the separation into two relaxations. These plots indicate that the critical size of cooperative motions n_1 is about 11 side chains.

The plots of R_e in Figure 6 indicate that the critical size n_{1K} of cooperative motion in the Konishi–Hatano model is about 13 side chains. This is very close to the value of n_1 estimated in the random copolymer model, suggesting that the sequence of side chains in the Konishi–Hatano model is similar to that in the random copolymer model. Since the sequence in the region under consideration is expected to be more random than that in the Konishi–Hatano model, we may determine the critical size to be about 11.

(ii) *Blend of PMLG and PpClBLG.* X-ray photographs of the blend showed two reflections corresponding to the spacings due to PMLG and P*p*ClBLG crystals, and a weak reflection corresponding to a mean value of these two reflections. The latter reflection indicates the existence of a crystalline region in which PMLG and P*p*ClBLG molecules are miscible. This crystalline region seems to be reflected by the dielectric properties. Since the degrees of polymerization of PMLG and P*p*ClBLG used are the same, we can use ϕ_m and ϕ_p instead of ϕ_{P_m} and ϕ_{P_p}. Estimated values of R_2 for the blends are plotted in Figure 7. It was found that the value of n_2 is 2.5. Taking into account the existence of PMLG and P*p*ClBLG crystals in the blend, this value is taken as a lower limit of n_2.

The value of $n_2=2.5$ suggests that if the fraction of 'P_p' side-chains in the shaded area of Figure 1c is more than 17% [$=(3-2.5)/3$], all side chains in this area are in the 'P_p' motional state. The corresponding value for the copolymer is 8% [$=1/(11+1)$], which is smaller than that for the blend. One of the reasons for this disagreement is that the 'P_p' side-chains in the blend are more localized than the '*p*' side-chains of the copolymers. We may thus conclude that the side chains of PMLG molecules surrounded by less than two P*p*ClBLG molecules exhibit the 'P_m' motional state, while the other side chains exhibit the 'P_p' motional state. These results do not conflict the results that the cooperative size of side-chain motion in the copolymer system is 11.

Effective Free-Volume of MLG Side-Chains

The reason that the relaxation related to the MLG side-chains in the blend did not shift to lower temperature, differing from the copolymers, can be explained in terms of the effective free-volume[20] of MLG side-chains and the coaxial two-phase model.[16] The radius of the side-chain region in the two-phase model determines the effective free-volume of

MLG side-chain. The steric effect due to the *p*ClBLG side-chains in the copolymer gives rise to an increase of the radius. Therefore, the effective free-volume of MLG side-chains will increase with increasing ϕ_p. In the case of polymers blend, however, this increase cannot be expected.

The effective free-volume was estimated from the inter-helix distance. The increase in this distance for the copolymer was evidenced by an X-ray photograph.[15] However, for the polymer blend, we observed no change in the spacing with the composition. The difference in free-volume change between the copolymer and the blend explains the difference in dielectric behavior between the two systems, and also indicates that the structure of α-helical poly(α-amino acid) in the solid state is well described by the coaxial two-phase model.

Comparison of Cooperative Motion in Poly(α-amino acid) with That in Amorphous Polymer

It is of interest to compare the cooperative motions of side chains of poly(α-amino acid)s with those of main chains of conventional amorphous polymers. The fact that only one glass-rubber relaxation is observed in vinyl-type copolymers[8,9] indicates that the number of monomer units involved in the cooperative main-chain motion is larger than that in the side-chain motion of poly(α-amino acid)s. The cooperative interaction is related to the intermolecular and intramolecular interactions and the latter comes largely from the chain connectivity. The effect of chain connectivity is not remarkable for the side chains of poly(α-amino acid), because the α-helical backbone is fixed to a rigid conformation.

CONCLUSION

The abrupt change in dielectric loss with the composition for copolymers of MLG and *p*ClBLG is caused by cooperative motions of the side chain. The critical size for the cooperative motions was about 11 side chains. This value was compared with the value for the polymer blend. Differences in dielectric properties between the copolymer and the blend were explained in terms of our models and the effective free-volume. It is reasonable to conclude that side-chain motions of poly(α-amino acid) involve a smaller number of structural units than main-chain motions of conventional amorphous polymer.

REFERENCES

1. J. E. Anderson, *J. Chem. Phys.*, **52**, 2821 (1970).
2. E. Helfand, *J. Chem. Phys.*, **69**, 1010 (1978); E. Helfand, Z. R. Wasserman, and T. A. Weber, *Macromolecules*, **13**, 526 (1980).
3. Y. Y. Gotlib, N. K. Balabaev, A. A. Darinskii, and I. M. Naelov, *Macromolecules*, **13**, 602 (1980).
4. G. Adam, *J. Chem. Phys.*, **43**, 662 (1965).
5. G. Adam and J. H. Gibbs, *J. Chem. Phys.*, **43**, 139 (1965).
6. R. J. Greet, *J. Chem. Phys.*, **45**, 2479 (1966).
7. N. Hill, W. E. Vaughan, A. H. Price, and M. Davis, "Dielectric Properties and Molecular Behavior," Van Nostrand Reinhold Company, London, 1969, Chapter 5.
8. Y. Kawamura, S. Nagai, J. Hirose, and Y. Wada, *J. Polym. Sci., A-2*, **7**, 1559 (1969).
9. S. Yagihara and S. Mashimo, *J. Polym. Sci., Polym. Phys. Ed.*, **19**, 1333 (1981).
10. S. Mashimo, S. Yagihara, and Y. Iwasa, *J. Polym. Sci., Polym. Phys. Ed.*, **16**, 1761 (1978).
11. A. Hiltner, *Macromolecules*, **5**, 446 (1972).
12. K. Adachi, Y. Hirose, and Y. Ishida, *J. Polym. Sci., Polym. Phys. Ed.*, **13**, 737 (1975).
13. A. Tsutsumi, K. Hikichi, T. Takahashi, Y. Yamashita, N. Matsushima, M. Kanke, and M. Kaneko, *J. Macromol. Sci., Phys.*, **B8**, 413 (1973).
14. N. Sasaki, H. Shimodate, Y. Yamashita, and K. Hikichi, *Polym. J.*, **11**, 983 (1979).
15. S. Yagihara and K. Hikichi, *Polym. J.*, **13**, 579 (1981).
16. N. Matsushima and K. Hikichi, *Polym. J.*, **10**, 437 (1978).
17. M. Chien, E. T. Samulski, and C. G. Wade, *Macromolecules*, **6**, 638 (1973).
18. T. Hiraoki, A. Tsutsumi, K. Hikichi, and M. Kaneko, *Polym. J.*, **8**, 524 (1976).
19. Y. Konishi and M. Hatano, *J. Polym. Sci., Polym. Chem. Ed.*, **14**, 2329 (1976).
20. A. K. Doolittle, *J. Appl. Phys.*, **22**, 1471 (1952); *ibid.*, **23**, 236 (1952).